

Tharsis as a consequence of Mars' dichotomy and layered mantle

Mark J. Wenzel,¹ Michael Manga,¹ and A. Mark Jellinek²

Received 17 December 2003; revised 16 January 2004; accepted 27 January 2004; published 25 February 2004.

[1] The two most striking features of the martian surface topography are the Tharsis rise and the crustal dichotomy. Closely associated with Tharsis are several large volcanoes, active in the geologically recent past, indicating a longevity of volcanic activity at Tharsis that is unique in the solar system. Using analogue laboratory experiments we examine the dynamical effects of the crustal dichotomy and a layered mantle on the thermal evolution of Mars. We show that in combination these two effects lead to the formation of a large-scale upwelling under the southern highlands that appears early and endures for many billions of years. The upwelling comprises several persistent narrow plumes, which can explain the long-lived Tharsis volcanoes. **INDEX TERMS:** 5455 Planetology: Solid Surface Planets: Origin and evolution; 5475 Planetology: Solid Surface Planets: Tectonics (8149); 5480 Planetology: Solid Surface Planets: Volcanism (8450); 8147 Tectonophysics: Planetary interiors (5430, 5724). **Citation:** Wenzel, M. J., M. Manga, and A. M. Jellinek (2004), Tharsis as a consequence of Mars' dichotomy and layered mantle, *Geophys. Res. Lett.*, *31*, L04702, doi:10.1029/2003GL019306.

1. Introduction

[2] The two largest and most enigmatic features of the martian surface are the crustal dichotomy and Tharsis. The crustal dichotomy is the nearly-hemispheric division that separates the Martian surface into northern and southern regions. The northern surface is topographically lower [Zuber *et al.*, 2000] and smoother [Smith *et al.*, 1999], and has thinner crust [Zuber *et al.*, 2000] than the southern surface. The dichotomy is among the oldest features on Mars [Tanaka, 1986; Frey *et al.*, 2002].

[3] Tharsis is a 30-million km² bulge rising ~10 km above the mean surface elevation [Phillips *et al.*, 2001]. Tharsis is old, with its bulk in place by the end of the Noachian [Phillips *et al.*, 2001], probably 3.5–3.8 Ga [Tanaka, 1986]. This feature is the site of the solar system's largest volcanoes, Olympus Mons and the Tharsis Montes, at least one of which (Arsia Mons) may have been active within the last 40 Myr [Hartmann *et al.*, 1999]. Volcanism has thus persisted for >3.5 Ga, a longevity in one location that is probably unique in the solar system.

[4] Here we show that two factors, in combination, allow for the formation and persistence of mantle plumes for billions of years: the presence of the dichotomy and a compositionally stratified mantle. We argue that such plumes can explain the longevity of volcanism at Tharsis.

¹Department of Earth and Planetary Science, University of California, Berkeley, California, USA.

²Department of Physics, University of Toronto, Toronto, Canada.

2. Effects of the Dichotomy and Arguments for a Layered Mantle

[5] As the martian crust is expected to be enriched in heat-producing elements relative to the mantle, the thicker crust in the highlands leads to higher temperatures at the crust-mantle interface, and therefore to a lower conductive heat flux from the mantle [Busse, 1978]. This insulating effect can greatly affect the dynamics of the mantle [e.g., Lenardic and Moresi, 2003].

[6] It has also been suggested that crystallization from an early magma ocean would lead to compositional layering of the martian mantle [Elkins-Tanton *et al.*, 2003; Kiefer, 2003]. While models of the mass distribution of Mars with a single mantle layer are unable to simultaneously match the Dreibus and Wänke [1985] compositional model, a chondritic bulk composition, and the observed moment of inertia factor [Bertka and Fei, 1998; Spohn *et al.*, 2001], the stratified model can satisfy these constraints [Elkins-Tanton *et al.*, 2003]. Furthermore, it has been inferred from studies of martian meteorites that the martian mantle is chemically heterogeneous [Halliday *et al.*, 2001], a constraint that can also be satisfied with a layered mantle [Kiefer, 2003].

[7] One explanation for the Tharsis Montes and Olympus Mons is that they are the products of long-lived mantle plumes [Carr, 1973]. The classic view of such plumes is that they form as a result of heat transfer into the base of the convecting mantle. The lack of an internally generated magnetic field on Mars, however, implies a low heat flux from the core into the mantle [Nimmo and Stevenson, 2000], though this is not enough to rule out the existence of plumes originating from the core-mantle boundary. In a compositionally layered mantle with negligible bottom heating the bottom layer can be a heat source for mantle plumes in the upper layer. Moreover, the interface between the two layers will also be deformed by the flow into topographically higher and lower regions; this topography can act to stabilize the locations of upwelling plumes [Jellinek and Manga, 2002].

3. Experimental Methods

[8] To investigate a dynamical link between the dichotomy, mantle layering, and volcanism associated with mantle plumes, we perform a series of analogue laboratory experiments with a fluid with temperature-dependent viscosity (corn syrup) (Figure 1). We choose an experimental approach because there are four aspects of this problem that, while amenable to experimental studies, in combination make a numerical investigation challenging. (1) We must resolve the dynamics of the sharp chemical and thermal interface [e.g., Tackley and King, 2003]. (2) The experiment must run for timescales equivalent to the whole of martian history [Schott *et al.*, 2001]. (3) The flow is three-dimensional and time-dependent. (4) There are large lateral viscosity variations over very small length scales. The experiments are limited by

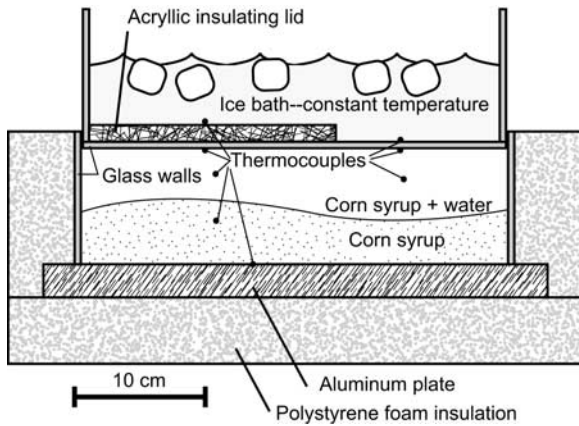


Figure 1. Experimental apparatus.

the boundary conditions they impose, including a Cartesian geometry and no-slip sidewalls. The experimental rheologies do not include plastic or elastic effects, and in these experiments, only local measurements of temperature, heat flux, and density can be made. However, from these local measurements global parameters such as the Rayleigh number and Nusselt number can be determined.

[9] We perform the experiments in a glass-walled, aluminum-floored tank of 32.7 cm by 32.7 cm by 7.85–8.45 cm interior dimension (aspect ratio ~ 4) (Figure 1). The top boundary condition is set to be at a constant temperature by an inset glass tank, filled with well-stirred ice water. To simulate the thicker highland crust, for some experiments 20%–100% of the floor of the inset tank is covered with a 1.27-cm thick acrylic insulating lid. The effective thermal conductivity of the insulated side is $\sim 40\%$ of that of the side with no insulating lid, equivalent to a crust about twice as thick under the southern highlands [Zuber *et al.*, 2000]. Working fluids are aqueous corn syrup solutions, with food dye added to the lower layer. Two opposite sides of the tank are insulated with 5.08-cm-thick polystyrene foam blocks. The two remaining sides are left open so that we can photograph and videotape the experiment. The experiments take one of two forms: (1) bottom heating and top cooling, or (2) secular cooling simulating internal heating [Schott *et al.*, 2001]. In the experiments with bottom heating, the fluids and the tank are initially at room temperature; the base of the tank is a hollow aluminum heat exchanger, through which hot

water is pumped. In contrast, in the experiments with secular cooling the tank base is insulated. The fluids and the tank base are separately warmed to 59–68°C and the fluids are then poured into the tank. We then bring the ice bath into contact with the top of the fluid, which results in thermal convection. The system cools over time as heat is lost to the ice bath. We quantify heat transfer during convection with timeseries of temperature and heat flux, measured with thermocouples and heat flux sensors on the tank roof and floor and thermocouple probes within the convecting interior.

4. Parameters

[10] We characterize our experiments with four non-dimensional parameters: the buoyancy number B , the Rayleigh number Ra , the viscosity ratio λ , and the fraction of the tank depth occupied by the lower layer, ϕ . The aspect ratio of the tank is fixed and the Reynolds number is always $\ll 1$. The variable parameters are defined such that $B = \Delta\rho_c/\rho\alpha\Delta T_i$, $Ra = \rho g\alpha\Delta T_i h^3/\kappa\mu$, $\lambda = \mu_{\text{lower}}/\mu_{\text{upper}}$, and $\phi = l/h$, where $\Delta\rho_c$, ρ , α , ΔT_i , g , ΔT_b , κ , h , μ , and l are compositional density difference, density of the upper layer, thermal expansivity, difference in interior temperatures between the two layers, gravity, difference in temperature between the floor of the tank and the ice bath, thermal diffusivity, total fluid depth, viscosity, and depth of the lower layer when the interface is flat, respectively. μ for the upper and lower layers is reported at the interior temperature of each layer. B is the ratio of chemical to thermal buoyancy forces and governs the height of interfacial topography and the amount of entrainment. In the cases simulating internal heating, B is initially high as the temperature difference between the fluids is small, decreases very rapidly and then more slowly, to some minimum value (always > 2) and then climbs again as the whole system cools and the temperature difference decreases. ΔT_i and $\Delta\rho_c$ averaged from the garnet segregation model of Elkins-Tanton *et al.* [2003], in which the lower mantle is enriched in alumina, imply an initial $B \approx 5.3$. Given the temporal evolution of B in the experiments a direct comparison to the theoretical result is difficult. The experiments, however, are well within the regime of $B \geq 1$, and thus the system is stably stratified [LeBars and Davaille, 2002]. λ also evolves, for the same reasons as B , but is always between one and ten throughout all

Table 1. Parameters for Experiments

Experiment	Ra_{max}	Duration (τ)	Lower layer depth fraction (ϕ)	Heating mode	Lid extent
1	1.1×10^5	Reached steady state	0.18	bottom	0
2	4.3×10^5	Reached steady state	0.16	bottom	0.6
3	3.6×10^5	Reached steady state	0.20	bottom	0.6
4	$>7.0 \times 10^5$	0.66	0.37	internal	0
5*	3.0×10^6	0.60	0.40	internal	0.6
6	5.9×10^6	0.58	0	internal	0.6
7	3.0×10^6	0.35	0.43	internal	0
8*	1.2×10^6	0.38	0.27	internal	0.6
9*	4.2×10^6	0.39	0.50	internal	0.6
10	1.1×10^5	0.45	0.72	internal	0.6
11	4.5×10^5	Reached steady state	0	bottom	0
12	6.0×10^5	Reached steady state	0	bottom	0.43
13	3.8×10^5	Reached steady state	0	bottom	0.2
14	6.4×10^5	Reached steady state	0	bottom	0.83
15	8.7×10^5	Reached steady state	0	bottom	1
16	7.5×10^5	Reached steady state	0	bottom	0.6

Asterisk indicates experiments in which an upwelling and stable plumes form under the insulating lid.

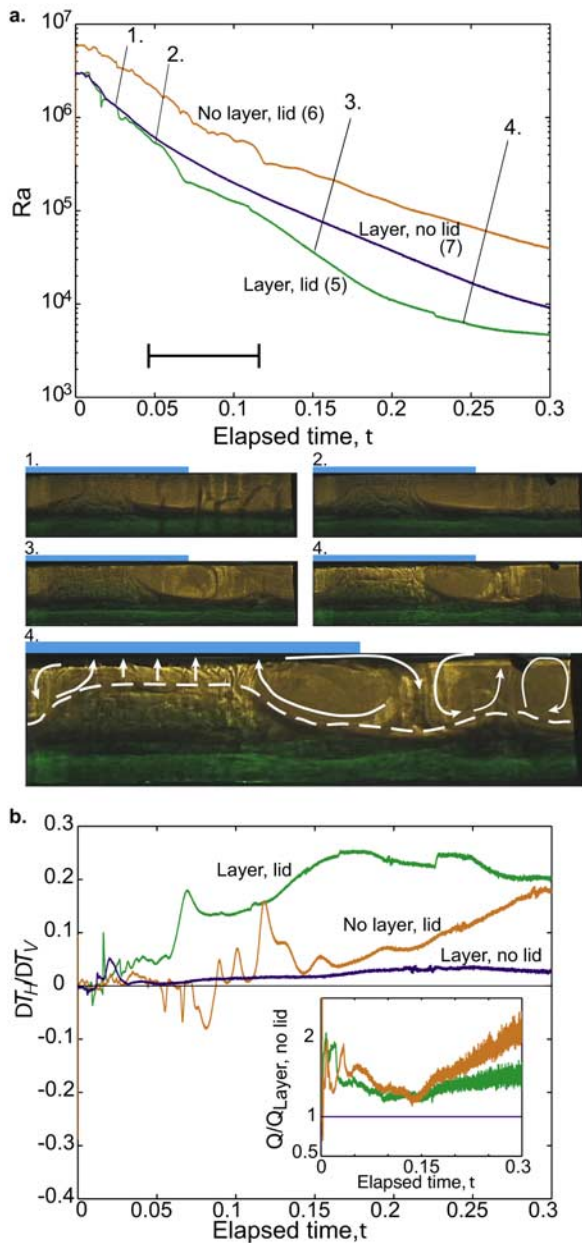


Figure 2. (A) Rayleigh number v. time for “layer, no lid” (blue), “no layer, lid” (orange), and “layer, lid” (green) cases. Time is reported as a fraction of the diffusion time, $\tau = h^2/\kappa$. The scale bar shows a range of times corresponding to the present day, based on the mantle diffusion timescale (0.047τ) and the time for the heat flux from the “layer, lid” case to decay by a factor of 3.3 (0.118τ) [Hauck and Phillips, 2002]. Shadowgraphs from the points in time marked 1–4 show flow and interface topography for the “layer, lid” case; the gray bar shows the extent and position of the insulating lid. Arrows on the larger picture at time 4 indicate flow direction; the dashed line indicates the interface between layers. (B) Horizontal temperature difference ΔT_H normalized to vertical temperature difference ΔT_V . Large ΔT_H starts to develop much earlier (0.01τ) for the layered case than for the nonlayered case (0.10τ). The inset figure shows the ratio of heat flux (Q) in each experiment to that of the “layer, no lid” case.

experiments.

[11] Absolute time in the experiments is scaled to time for martian evolution in two ways. First, time is reported as a fraction of the diffusion time, $\tau = h^2/\kappa$. Martian time of the present day is 0.047τ . The diffusion timescale is appropriate for a cooling system with no internal heat production within the mantle, and thus represents one endmember of martian mantle models. The second timescale is the length of time required for the heat flux in the experiment to decline by a factor of ~ 3.3 , the amount of heat flux decrease calculated for Mars by a thermal evolution model that includes internal heating and crust formation [Hauck and Phillips, 2002]. For large Ra, it is reasonable to assume surface heat flow is roughly proportional to $Ra^{1/3}$. Thus, it will be reduced by a factor of 3.3 when Ra has decreased by a factor of 3.3^3 , or about 36.

5. Results and Discussion

[12] Parameters for sixteen experiments are presented in Table 1. We focus first on the results from three experiments, all simulating internal heating, in order to illustrate the main features of the interaction between the dichotomy (variation in crustal thickness) and a layered mantle. The reference case is a layered mantle system with a uniform upper boundary condition (called the “layer, no lid” case); the second is an experiment with a uniform convecting fluid and an insulating lid (“no layer, lid”); the third is a layered system with an insulating lid (“layer, lid”).

[13] At the start of all experiments, transient, short-lived downwellings initiate at the surface on contact with the ice bath. As the experiments progress, the interior cools, the viscosity increases, and consequently Ra decreases (Figure 2a). Beyond these similarities, the style of flow varies considerably depending on the presence or absence of the insulating lid and compositional layering. In the “layer, lid” case, starting at 0.011τ , a large swell forms on the interface between the two layers, under the insulating lid. The swell has an arcuate ridge at its top, as in Jellinek and Manga [2002], off of which rise four to

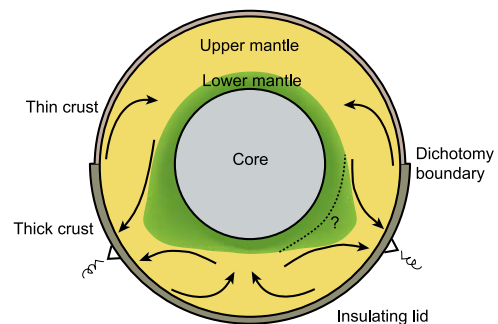


Figure 3. Martian mantle structure. Arrows indicate flow direction. The thicker crust of the highlands forms an insulating lid, under which a broad swell (or perhaps more than one swell, in spherical geometry) forms. Narrow upwelling plumes rising from the top of the swell cause persistent volcanism such as that observed at Tharsis and Elysium.

five plumes. Around the swell is a trough formed by the descent of cool material. The swell reaches its greatest extent at $\sim 0.12 \tau$, when its width is approximately twice the upper layer depth. As Ra decreases, so do convective velocities and, hence, the viscous stresses that maintain the topography on the interface. The maximum height of the topography therefore diminishes over the course of the experiment. In Figure 2a, frames from the time-lapse video show the formation of the swell and its size and persistence through the length of the experiment (equivalent to 25–64 Gyr) and almost three orders of magnitude of Ra . In the “layer, no lid” case, upwelling and downwelling plumes form quickly and remain in approximately the same location for the length of the experiment. The upwellings and downwellings develop into stable convection cells of aspect ratio ~ 1 . In the “no layer, lid” case, following the formation of the initial convective instabilities across the whole surface, broad upwellings form at the edges of the tank at 0.05τ , spread across the tank roof, and then form strong stable downwellings at their edges. At 0.18τ new upwellings, replacing the edge upwellings, form under the center of the lid.

[14] The large-scale flow responsible for the broad swell in the “layer, lid” case is driven by a lateral temperature difference in the interior of the upper layer (ΔT_H) between warm fluid beneath the lid and the cool fluid on the no-lid side. ΔT_H becomes large in both cases with a lid (Figure 2b). However, the layered case begins to develop large ΔT_H early (0.01τ); it develops much later in the non-layered case (0.10τ). The total surface heat flux in each experiment is measured and their ratios are compared (Figure 2b, inset). The effect of the insulating lid is to increase heat flux from the system by raising the internal temperature and therefore lowering viscosity and increasing Ra . Of the two cases with lids, the non-layered case has a higher heat flux than the layered case. The presence of a lower layer reduces the depth and therefore Ra of the upper layer, resulting in lower convective velocities and hence less heat transfer. Indeed, lower heat transfer for a layered martian mantle is consistent with the absence of an internally-generated magnetic field since the Noachian [Nimmo and Stevenson, 2000].

[15] Our initial Ra are 10^5 – 10^6 , which are lower than values calculated for Mars by other means [Kiefer, 2003]. However, the pattern of flow we observe in cases with an insulating lid is independent of Ra over the range 10^4 – 10^6 . When the insulating lid is present, the lateral temperature difference determines the large-scale flow pattern, a result that should not change at higher Ra . In fact, at higher Ra the convective velocities and therefore the deformation of the interface will be larger, and plumes should be even more stable [Jellinek and Manga, 2002].

[16] One challenge to the proposed model is that the center of the upwelling in the experiments is below the insulating lid, while on Tharsis and the other large volcanic center, Elysium, are centered close to the dichotomy boundary. We are currently investigating whether a spherical geometry affects plume locations.

[17] From these and the other 13 experiments (Table 1), some additional conclusions can be reached: (1) The effect of the insulating lid is much smaller in bottom-heated cases than internally-heated cases. There is no evidence for large-scale flow structures in the bottom-heated cases with

layering. (2) Independent of the fraction of the tank depth occupied by the lower layer, horizontal temperature differences develop and persist in all cases with an insulating lid. Single large swells formed on the interface for all cases with a lower layer fraction less than 0.7. In experiment 10, which had a lower layer depth fraction of 0.72, the topography on the interface had three ridges parallel to the lid edge.

6. Conclusion

[18] A two-layered mantle on Mars reconciles constraints on the moment of inertia factor, a chondritic bulk composition, and the observed heterogeneity in martian meteorite chemistry. The crustal dichotomy creates a variable-heat-flux upper boundary condition on the convecting mantle. Our experiments show that in combination, layering and the dichotomy result in upwellings under the thicker crust that form early and persist for billions of years, as illustrated schematically in Figure 3. Assuming that persistent mantle upwelling leads to volcanism, our work thus shows that the effects of layering and the dichotomy lead to a self-consistent explanation of the early formation and billion-year persistence of volcanism on Tharsis, even in the absence of bottom heating.

[19] **Acknowledgments.** We thank NSF, NSERC and CIAR for support, and S. Hauck, L. Elkins-Tanton and D. Stegman for suggestions and A. Lenardic, J. Sanders and H. Gonnermann for lab help.

References

- Bertka, C. M., and Y. Fei (1998), Density profile of an SNC model martian interior and the moment-of-inertia factor of Mars, *Earth Planet. Sci. Lett.*, *157*, 79–88.
- Busse, F. H. (1978), A model of time-periodic mantle flow, *Geophys. J. R. Astron. Soc.*, *52*, 1–12.
- Carr, M. H. (1973), Volcanism on Mars, *J. Geophys. Res.*, *78*, 4049–4062.
- Dreibus, G., and H. Wänke (1985), Mars: A volatile-rich planet, *Meteoritics*, *20*, 367–382.
- Elkins-Tanton, L. T., et al. (2003), A model for martian magma ocean crystallization and overturn, *Meteoritics and Planetary Science*, *38*, 1753–1772.
- Frey, H. V., et al. (2002), Ancient lowlands on Mars, *Geophys. Res. Lett.*, *29*(10), 1384, doi:10.1029/2001GL013832.
- Halliday, A. N., et al. (2001), The accretion, composition, and early differentiation of Mars, *Space Sci. Rev.*, *96*, 197–230.
- Hartmann, W. K., et al. (1999), Evidence for recent volcanism on Mars from crater counts, *Nature*, *397*, 586–589.
- Hauck, S. A., and R. J. Phillips (2002), Thermal and crustal evolution of Mars, *J. Geophys. Res.*, *107*(E7), 5052, doi:10.1029/2001JE001801.
- Jellinek, A. M., and M. Manga (2002), The influence of a chemical boundary layer on the fixity, spacing, and lifetime of mantle plumes, *Nature*, *418*, 760–763.
- Kiefer, W. S. (2003), Melting in the martian mantle: Shergottite formation and implications for present-day mantle convection on Mars, *Meteoritics and Planetary Science*, *38*, 1815–1832.
- Le Bars, M., and A. Davaille (2002), Stability of thermal convection in two superimposed miscible viscous fluids, *J. Fluid Mech.*, *479*, 339–363.
- Lenardic, A., and L. Moresi (2003), Thermal convection below a conducting lid of variable extent: Heat flow scalings and two-dimensional, infinite Prandtl number numerical simulations, *Phys. Fluids*, *15*, 455–466.
- Nimmo, F., and D. J. Stevenson (2000), Influence of early plate tectonics on the thermal evolution and magnetic field of Mars, *J. Geophys. Res.*, *105*(E5), 11,969–11,979.
- Phillips, R. J., et al. (2001), Ancient geodynamics and global-scale hydrology on Mars, *Science*, *291*, 2587–2591.
- Schott, B., et al. (2001), Focussed time-dependent martian volcanism from chemical differentiation coupled with variable thermal conductivity, *Geophys. Res. Lett.*, *28*(22), 4271–4274.

- Smith, D. E., et al. (1999), The global topography of Mars and implications for surface evolution, *Science*, 284, 1495–1503.
- Spohn, T., et al. (2001), Geophysical constraints on the evolution of Mars, *Space Sci. Rev.*, 96, 231–262.
- Tackley, P. J., and S. D. King (2003), Testing the tracer ratio method for modeling active compositional fields in mantle convection simulations, *Geochem. Geophys. Geosyst.*, 4(4), 8302, doi:10.1029/2001GC00214.
- Tanaka, K. L. (1986), The stratigraphy of Mars, *J. Geophys. Res.*, 91, E139–E158.
- Zuber, M. T., et al. (2000), Internal structure and early thermal evolution of Mars from Mars Global Surveyor Topography and Gravity, *Science*, 287, 1788–1793.
-
- A. M. Jellinek, Department of Physics, University of Toronto, Toronto M5S 1A7, Canada.
- M. Manga and M. J. Wenzel, Department of Earth and Planetary Science, University of California, Berkeley, CA 94720, USA. (manga@seismo.berkeley.edu)